Group 5 Imido Complexes Derived from Diamido-Pyridine Ligands

Stephen M. Pugh,[†] Alexander J. Blake,[‡] Lutz H. Gade,*[,§] and Philip Mountford*[,†]

Inorganic Chemistry Laboratory, University of Oxford, South Parks Road, Oxford OX1 3QR, U.K., School of Chemistry, University of Nottingham, Nottingham, NG7 2RD, U.K., and Laboratoire de Chimie Organométallique et de Catalyse (CNRS UMR 7513), Institut Le Bel, Université Louis Pasteur, 4, rue Blaise Pascal, 67000 Strasbourg, France

Received March 6, 2001

Reaction of the vanadium(V) imide [V(NAr)Cl_3(THF)] (Ar = 2,6-$C_6H_3{}^iPr_2$) with the diamino-pyridine derivative MeC(2-C_5H_4N)($CH_2NHSiMe_2{}^tBu$)$_2$ (abbreviated as $H_2N'_2N_{py}$) gave modest yields of the vanadium(IV) species [V(NAr)($H_3N'N''N_{py}$)Cl_2] (**1** where $H_3N'N''N_{py}$ = MeC(2- C_5H_4N)(CH_2NH_2)($CH_2NHSiMe_2{}^tBu$) in which the original $H_2N'_2N_{py}$ has effectively lost $SiMe_2{}^tBu$ (as $ClSiMe_2{}^tBu$) and gained an H atom. Better behaved reactions were found between the heavier Group 5 metal complexes [M(NR)Cl_3(py)$_2$] (M = Nb or Ta, R = ^{t}Bu or Ar) and the dilithium salt $Li_2[N_2N_{py}]$ (where $H_2N_2N_{py}$ = MeC(2-C_5H_4N)($CH_2NHSiMe_3$)$_2$), and these yielded the six-coordinate M(V) complexes [M(NR)Cl(N_2N_{py})(py)] (M = Nb, R = ^{t}Bu **2**; M = Ta, R = ^{t}Bu **3** or Ar **4**). The compounds **2**−**4** are fluxional in solution and undergo dynamic exchange processes via the corresponding five-coordinate homologues [M(NR)Cl(N_2N_{py})]. Activation parameters are reported for the complexes **2** and **3**. In the case of **2**, high vacuum tube sublimation afforded modest quantities of [Nb(N^tBu)Cl(N_2N_{py})] (**5**). The X-ray crystal structures of the four compounds **1**, **2**, **3**, and **4** are reported.

Introduction

The chemistry of transition metal imido complexes (containing the NR ligand, where R is typically a hydrocarbyl group) has continued to attract considerable attention, particularly over the last 15 years.[1−8] The syntheses, reactivity, and bonding of such complexes in a wide variety of supporting ligand environments continues to be explored. In our groups we have recently been interested in using the diamido-pyridine and diamido-amine ligands MeC(2-C_5H_4N)(CH_2NSiMe_2R)$_2$ (abbreviated as N_2N_{py} for R = Me or N'_2N_{py} for R = ^{t}Bu)[9,10] and $Me_3SiN(CH_2CH_2NSiMe_3)_2$ (abbreviated as N_2N_{am})[11,12] as flexible and versatile supporting environments in imido chemistry.[8] Employing these hemi-labile ligands we have reported on the synthesis and structures of a family of Group 4 complexes of the types **I**, **II**, and **III** as shown in Chart 1.[13−15] These have reactive M=NR linkages which undergo a wide range of coupling reactions with many unsaturated organic substrates including the following: RNC, MeCN, ^{t}BuCP, ArNCO, RC_2Me, and $RCHCCH_2$.[13,16−19] Many of these transformations were the first, or among the first, of their type in transition metal imido chemistry.

To develop this successful area of work, we recently described attempts to use the diamido-amine ligand N_2N_{am} in Group 5 imido chemistry,[15] but in our efforts to prepare Group 5 analogues of the compounds **III** (Chart 1), we obtained mixtures of ill-behaved oils and ligand decomposition products (**IV** and **V**). In a more recently initiated project we found that well-defined Group 5 imides could be obtained using a chelating

* To whom correspondence should be addressed. Lutz H. Gade e-mail: gade@chimie.u-strasbg.fr. Philip Mountford e-mail: philip.mountford@chemistry.oxford.ac.uk. Fax: +44 1865 272690

[†] University of Oxford.

[‡] University of Nottingham.

[§] Université Louis Pasteur.

(1) Nugent, W. A.; Mayer, J. M. *Metal−Ligand Multiple Bonds*; Wiley-Interscience: New York, 1988.

(2) Chisholm, M. H.; Rothwell, I. P. *Comprehensive Coordination Chemistry*; Wilkinson, G., Gillard, R. D., McCleverty, J. A., Eds.; Pergamon Press: Oxford, 1987; Vol. 2.

(3) Wigley, D. E. *Prog. Inorg. Chem.* **1994**, *42*, 239.

(4) Mountford, P. *Chem. Commun.* **1997**, 2127.

(5) Sharp, P. R. *J. Chem. Soc., Dalton Trans.* **2000**, 2647.

(6) For applications of imido complexes in olefin polymerisation catalysis see: Coles, M. P.; Dalby, C. I.; Gibson, V. C.; Clegg, W.; Elsegood, M. R. J. *J. Chem. Soc., Chem. Commun.* **1995**, 1709; Chan, M. C. W.; Chew, K. C.; Dalby, C. I.; Gibson, V. C.; Kohlmann, A.; Little, I. R.; Reed, W. *Chem. Commun.* **1998**, 1673.

(7) For applications of imido complexes in ring opening metathesis polymerisation see: Schrock, R. R. *Acc. Chem. Res.* **1990**, *23*, 158; Gibson, V. C. *Adv. Mater.* **1994**, *6*, 37.

(8) For a review of imido complexes with diamido-donor ligands see: Gade, L. H.; Mountford, P. *Coord. Chem. Rev.*, in press. For a review of the chemistry of diamido-donor ligands in general see: Gade, L. H. *Chem. Commun.* **2000**, 173.

(9) Friedrich, S.; Schubart, M.; Gade, L. H.; Scowen, I. J.; Edwards, A. J.; McPartlin, M. *Chem. Ber.* **1997**, *130*, 1751.

(10) Galka, C. H.; Trösch, D. J. M.; Schubart, M.; Gade, L. H.; Radojevic, S.; Scowen, I. J.; McPartlin, M. *Eur. J. Inorg. Chem.* **2000**, 2577.

(11) Cloke, F. G. N.; Hitchcock, P. B.; Love, J. B. *J. Chem. Soc., Dalton Trans.* **1995**, 25.

(12) Clark, H. C. S.; Cloke, F. G. N.; Hitchcock, P. B.; Love, J. B.; Wainwright, A. P. *J. Organomet. Chem.* **1995**, *501*, 333.

(13) Blake, A. J.; Collier, P. E.; Gade, L. H.; McPartlin, M.; Mountford, P.; Schubart, M.; Scowen, I. J. *Chem. Commun.* **1997**, 1555.

(14) Blake, A. J.; Collier, P. E.; Gade, L. H.; Lloyd, J.; Mountford, P.; Pugh, S. M.; Schubart, M.; Skinner, M. E. G.; Trösch, D. J. M. *Inorg. Chem.* **2001**, *40*, 870.

(15) Pugh, S. M.; Clark, H. S. C.; Love, J. B.; Blake, A. J.; Cloke, F. G. N.; Mountford, P. *Inorg. Chem.* **2000**, *39*, 2001.

(16) Bashall, A.; Collier, P. E.; Gade, L. H.; McPartlin, M.; Mountford, P.; Trösch, D. T. *Chem. Commun.* **1998**, 2555.

(17) Cloke, F. G. N.; Hitchcock, P. B.; Nixon, J. F.; Wilson, D. J.; Mountford, P. *Chem. Commun.* **1999**, 661.

(18) Pugh, S. M.; Trösh, D. J. M.; Wilson, D. J.; Bashall, A.; Cloke, F. G. N.; Gade, L. H.; Hitchcock, P. B.; McPartlin, M.; Nixon, J. F.; Mountford, P. *Organometallics* **2000**, *19*, 3205.

(19) Bashall, A.; Gade, L. H.; McPartlin, M.; Mountford, P.; Pugh, S. M.; Radojevic, S.; Schubart, M.; Scowen, I. J.; Trösch, D. J. M. *Organometallics* **2000**, *19*, 4784.

10.1021/ic0102541 CCC: $20.00
Published on Web 06/30/2001

Chart 1

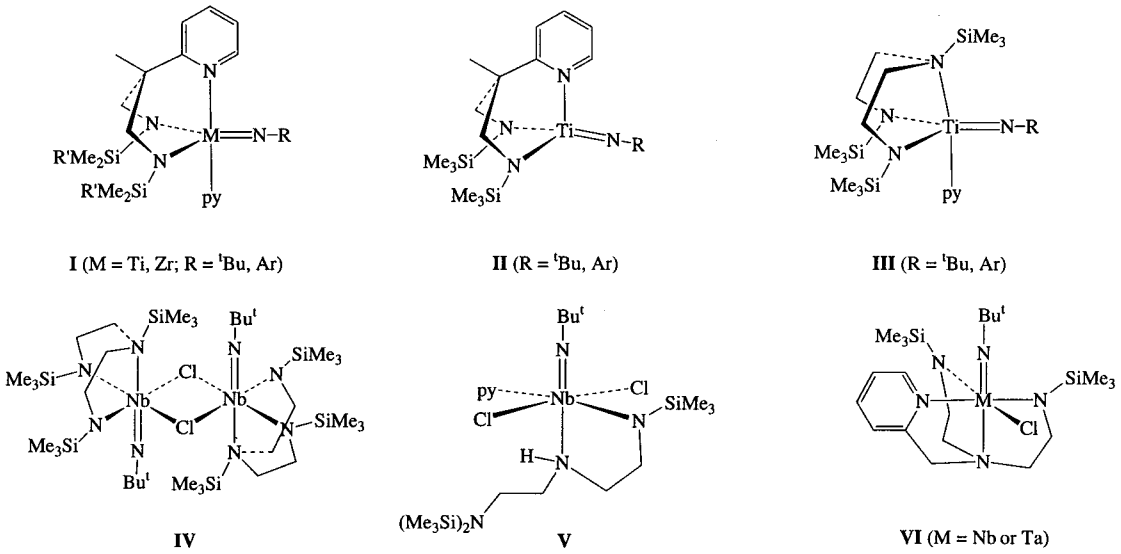

diamido-amine-pyridine ligand as shown in **VI**.[20] Here we report the synthesis of Group 5 imido complexes of the diamido-pyridine ligand N_2N_{py} and its *tert*-butyl homologue N'_2N_{py}.

Experimental Section

General Methods and Instrumentation. All manipulations were carried out using standard Schlenk line or drybox techniques under an atmosphere of argon or of dinitrogen. Solvents were predried over activated 4A molecular sieves and were refluxed over appropriate drying agents under a dinitrogen atmosphere and collected by distillation. Deuterated solvents were dried over potassium (C_6D_6) or calcium hydride (CD_2Cl_2), distilled under reduced pressure, and stored under dinitrogen in Teflon valve ampules. NMR samples were prepared under dinitrogen in 5 mm Wilmad 507-PP tubes fitted with J. Young Teflon valves. ^{1}H, ^{13}C-{^{1}H}, and ^{13}C NMR spectra were recorded on Bruker AM 300 and DPX 300 and Varian Unity Plus 500 spectrometers. ^{1}H and ^{13}C assignments were confirmed when necessary with the use of DEPT-135, DEPT-90, and two-dimensional ^{1}H-^{1}H and ^{13}C-^{1}H NMR experiments. All spectra were referenced internally to residual protio-solvent (^{1}H) or solvent (^{13}C) resonances and are reported relative to tetramethylsilane ($\delta = 0$ ppm). Chemical shifts are quoted in δ (ppm) and coupling constants in Hertz. Infrared spectra were prepared as Nujol mulls between CsBr or NaCl plates and were recorded on Perkin-Elmer 1600 and 1710 series, Nicolet Avatar 360, or Mattson Polaris FTIR spectrometers. Infrared data are quoted in wavenumbers (cm^{-1}). EPR spectra were recorded at room temperature on a Bruker EMX 6/1 RES EPR spectrometer. Mass spectra were recorded on an AEI MS902 mass spectrometer. Elemental analyses were carried out by the analysis laboratories of these departments. NMR assignments for **2**−**5** assume the following numbering scheme for the pyridyl group of N_2N_{py}:

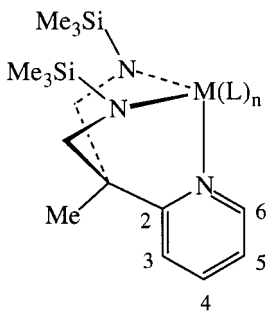

Literature Preparations. $H_2N_2N_{py}$,[9] $H_2N'_2N_{py}$,[10] $Li_2[N_2N_{py}]$,[10] [M(N^{t}Bu)Cl$_3$(py)$_2$] (M = Nb, Ta),[21] [Ta(NAr)Cl$_3$(py)$_2$],[22] and [V(NAr)Cl$_3$(thf)][23] were prepared according to literature methods.

[V(NAr)Cl$_2$(H$_3$N′N″N$_{py}$)] (1). A solution of $H_2N'_2N_{py}$ (0.296 g, 0.75 mmol) and Et_3N (0.196 g, 1.94 mmol) in diethyl ether (3 mL) was added to a solution of [V(N-2,6-C$_6$H$_3$^{i}Pr$_2$)Cl$_3$(thf)] (0.304 g, 0.75 mmol) in diethyl ether (10 mL) at −45 °C. The resulting brown solution was allowed to warm slowly to room temperature and was stirred for 5 h. It was then filtered and the residues were washed with diethyl ether (3 × 10 mL), the washings being added to the reaction solution. After standing at room temperature for 48 h, red-brown X-ray diffraction quality crystals of [V(NAr)Cl$_2$(HN′N″N$_{py}$)] (**1**) formed from the solution. These were filtered off and dried under reduced pressure. Yield: 0.050 g (12%). EPR: *g*-factor = 1.982, hyperfine coupling = 90.9091 G (thf, 298 K). EI mass spectrum: *m*/*z* = 177 [M$^+$ − V(N-2,6-C$_6$H$_3$^{i}Pr$_2$)Cl$_2$CH$_2$NH$_2$Me$_2$], *m*/*z* = 162 [M$^+$ − V(N-2,6-C$_6$H$_3$^{i}Pr$_2$)Cl$_2$-CH$_2$NH$_2$Me$_3$]. IR (CsBr plates, Nujol, cm^{-1}): 3349 (w), 3236 (m), 3158 (w), 1731 (w), 1603 (s), 1572 (w), 1323 (w), 1257 (s), 1096 (m), 1035 (s), 934 (w), 860 (m), 829 (s), 798 (w), 780 (m), 754 (s), 712 (m), 660 (w), 635 (w), 610 (w), 552 (w), 465 (w), 436 (w), 417 (w) cm^{-1}. Anal. Found (calculated for $C_{27}H_{46}Cl_2N_4SiV$): C 56.1 (56.2), H 8.4 (8.0), N 9.5 (9.7)%.

[Nb(N^{t}Bu)Cl(N$_2$N$_{py}$)(py)] (2). To a mixture of solid [Nb(N^{t}Bu)Cl$_3$(py)$_2$] (1.568 g, 3.66 mmol) and solid $Li_2[N_2N_{py}]$ (1.176 g, 3.66 mmol) was added cold (7 °C) benzene (30 mL). The resulting brown solution was stirred at room temperature for 4 h before being filtered. The insolubles were dried under reduced pressure and extracted into dichloromethane (2 × 20 mL) to provide a red-brown solution. This was filtered and the volatiles removed under reduced pressure leaving a yellow-brown solid. The solid was washed with diethyl ether (3 × 5 mL) and dried under reduced pressure to provide [Nb(N^{t}Bu)Cl(N$_2$N$_{py}$)(py)] (**2**) as a yellow powder. Yield: 1.328 g (62%). Yellow crystals of **2** suitable for X-ray diffraction were prepared by slow cooling of a saturated solution of **2** in toluene from 100 °C to room temperature over 10 h. ^{1}H NMR (CD_2Cl_2, 300.1 MHz, 298 K): 8.77 (2 H, dt, ^3J (*o*-H*m*-H) = 4.8 Hz, ^4J (*o*-H*p*-H) = 1.8 Hz, *o*-NC$_5$H$_5$), 8.18 (1 H, dd, ^3J (H^{6}H^5) = 5.7 Hz, ^4J (H^{6}H^4) = 1.5 Hz, H^6), 7.74 (2 × 1 H, 2 × overlapping m, H^4, and *p*-NC$_5$H$_5$), 7.47 (1 H, dt, ^3J (H^{3}H^4) = 8.1 Hz, ^4J (H^{3}H^5) = 0.9 Hz, H^3), 7.21 (2 H, apparent t, apparent J = 5.0 Hz, *m*-NC$_5$H$_5$), 6.92 (1 H, apparent t, apparent J = 6.9 Hz, H^5), 3.62 (2 H, d, ^2J = 12.7 Hz, CH$_2$), 3.45 (2 H, d, ^2J = 12.7 Hz, CH$_2$), 1.52 (3 H,

(20) Skinner, M. E. G.; Cowhig, D. A.; Mountford, P. *Chem. Commun.* **2000**, 1167.

(21) Sundermeyer, J.; Putterlik, J.; Foth, M.; Field, J. S.; Ramesar, N. *Chem. Ber.* **1994**, *127*, 1201.

(22) Chao, Y.-W.; Wexler, P. A.; Wigley, D. E. *Inorg. Chem.* **1989**, *28*, 3860.

(23) Devore, D. D.; Lichtenhan, J. D.; Takusagawa, F.; Maatta, E. A. *J. Am. Chem. Soc.* **1987**, *109*, 7408.

s, Me of N_2N_{py}), 1.45 (9 H, s, ^{t}Bu), 0.12 (18 H, s, $SiMe_3$). ^{1}H NMR (CD_2Cl_2, 300.1 MHz, 218 K): 8.06 (1 H, dd, ^3J (H^6H^5) = 5.7 Hz, ^4J (H^6H^4) = 1.5 Hz, H^6), 7.73 (2 × 1 H, 2 × overlapping m, H^4 and *p*-NC_5H_5), 7.46 (1 H, d, ^3J (H^3H^4) = 8.1 Hz, H^3), 7.21 (2 H, broad s, *m*-NC_5H_5), 6.91 (1 H, apparent t, apparent J = 6.5 Hz, H^5), 3.57 (1 H, d, ^2J = 13.2 Hz, CH_2), 3.54 (1 H, d, ^2J = 13.4 Hz, CH_2), 3.42 (1 H, d, ^2J = 13.2 Hz, CH_2), 3.36 (1 H, d, ^2J = 13.2 Hz, CH_2), 1.48 (3 H, s, Me of N_2N_{py}), 1.39 9 H, s, ^{t}Bu), 0.21 (9 H, s, $SiMe_3$), −0.09 (9 H, s, $SiMe_3$), not observed: *o*-NC_5H_5. ^{13}C-{^{1}H} NMR (CD_2Cl_2, 75.5 MHz, 218 K): 163.6 (C^2), 153.3 (*o*-NC_5H_5), 149.4 (C^6), 139.0 (C^4), 138.3 (*p*-NC_5H_5), 123.3 (*m*-NC_5H_5), 121.1 (C^5), 119.4 (C^3), 66.9 (N*C*Me$_3$), 62.7 (*C*H_2NSiMe$_3$), 62.5 (*C*H_2NSiMe$_3$), 50.0 (*C*(CH_2NSiMe$_3$)$_2$), 32.0 (NC*Me*$_3$), 24.6 (Me of N_2N_{py}), 1.8 (Si*Me*$_3$), 1.6 (Si*Me*$_3$). IR (CsBr plates, Nujol, cm^{-1}): 1601 (s), 1571 (w), 1483 (m), 1398 (w), 1294 (w), 1243 (s), 1216 (m), 1163 (w), 1161 (w), 1137 (w), 1116 (m), 1089 (m), 1075 (w), 1061 (m), 1046 (s), 1015 (m), 1008 (w), 961 (m), 910 (s), 841 (s), 809 (s), 785 (s), 756 (s), 704 (m), 641 (w), 628 (w), 599 (m), 558 (w), 535 (w), 486 (m), 446 (w), 430 (w) cm^{-1}. Anal. Found (calculated for $C_{24}H_{43}ClN_5NbSi_2$): C 49.0 (49.2), H 7.7 (7.4), N 12.4 (12.0)%.

[Ta(N^{t}Bu)Cl(N_2N_{py})(py)] (3). To a mixture of solid [Ta(N^{t}Bu)Cl_3(py)$_2$] (0.500 g, 0.96 mmol) and solid $Li_2[N_2N_{py}]$ (0.310 g, 0.96 mmol) was added cold (7 °C) benzene (25 mL). The resulting brown solution was stirred at room temperature for 5 h before being filtered. The insolubles were dried under reduced pressure and extracted into dichloromethane (2 × 15 mL) to provide a pale yellow solution. This was filtered and the volatiles removed under reduced pressure leaving a pale orange solid. The solid was washed with diethyl ether (2 × 3 mL) and dried under reduced pressure to provide **3** as a white powder. Yield: 0.215 g (33%). Pale yellow crystals of **3** suitable for X-ray diffraction were prepared by slow cooling of a saturated solution of **3** in toluene from 120 °C to room temperature over 72 h. ^{1}H NMR (CD_2Cl_2, 300.1 MHz, 298 K): 8.84 (2 H, d, ^3J (*o*-H*m*-H) = 5.0 Hz, *o*-NC_5H_5), 8.26 (1 H, dd, ^3J (H^6H^5) = 5.7 Hz, ^4J (H^6H^4) = 1.8 Hz, H^6), 7.77 (2 × 1 H, 2 × overlapping m, H^4 and *p*-NC_5H_5), 7.48 (1 H, dt, ^3J (H^3H^4) = 7.9 Hz, ^4J (H^3H^5) = 1.1 Hz, H^3), 7.24 (2 H, apparent t, apparent J = 5.0 Hz, *m*-NC_5H_5), 6.94 (1 H, apparent t, apparent J = 6.0 Hz, H^5), 3.70 (2 H, d, ^2J = 12.1 Hz, CH_2), 3.59 (2 H, d, ^2J = 12.5 Hz, CH_2), 1.47 (3 H, s, Me of N_2N_{py}), 1.39 (9 H, s, ^{t}Bu), 0.07 (18 H, broad s, $SiMe_3$). ^{1}H NMR (CD_2Cl_2, 300.1 MHz, 223 K): 8.17 (1 H, d, ^3J (H^6H^5) = 5.5 Hz, H^6), 7.77 (1 H, overlapping m, H^4), 7.77 (1 H, overlapping m, *p*-NC_5H_5), 7.48 (1 H, d, ^3J (H^3H^4) = 8.1 Hz, H^3), 7.25 (2 H, broad s, *m*-NC_5H_5), 6.96 (1 H, apparent t, apparent J = 6.2 Hz, H^5), 3.67 (1 H, d, ^2J = 12.5 Hz, CH_2), 3.64 (1 H, d, ^2J = 12.3 Hz, CH_2), 3.55 (1 H, d, ^2J = 12.9 Hz, CH_2), 3.50 (1 H, d, ^2J = 12.7 Hz, CH_2), 1.44 (3 H, s, Me of N_2N_{py}), 1.34 (9 H, s, ^{t}Bu), 0.21 (9 H, s, $SiMe_3$), −0.11 (9 H, s, $SiMe_3$), not observed: *o*-NC_5H_5. ^{13}C-{^{1}H} NMR (CD_2Cl_2, 75.5 MHz, 223 K): 164.2 (C^2), 154.0 (*o*-NC_5H_5), 149.7 (C^6), 139.3 (C^4), 138.6 (*p*-NC_5H_5), 123.6 (*m*-NC_5H_5), 121.5 (C^5), 119.5 (C^3), 65.0 (N*C*Me$_3$), 61.8 (*C*H_2NSiMe$_3$), 61.7 (*C*H_2NSiMe$_3$), 49.8 (*C*(CH_2NSiMe$_3$)$_2$), 33.4 (NC*Me*$_3$), 24.3 (Me of N_2N_{py}), 1.9 ($SiMe_3$), 1.8 ($SiMe_3$). IR: (CsBr plates, Nujol, cm^{-1}): 1603 (s), 1571 (w), 1483 (m), 1385 (w), 1295 (w), 1253 (s), 1217 (m), 1160 (w), 1155 (w), 1134 (w), 1091 (w), 1076 (w), 1062 (w), 1047 (s), 1016 (m), 1009 (w), 962 (m), 918 (s), 848 (s), 782 (m), 757 (m), 703 (m), 642 (w), 630 (w), 599 (m), 560 (w), 532 (w), 488 (m), 445 (w), 431 (w) cm^{-1}. Anal. Found (calculated for $C_{24}H_{43}ClN_5Si_2Ta$): C 42.3 (42.8), H 7.0 (6.4), N 9.4 (10.4)%.

[Ta(NAr)Cl(N_2N_{py})(py)] (4). To a mixture of solid [Ta(N-2,6-$C_6H_3{}^i$Pr$_2$)Cl_3(py)$_2$] (0.414 g, 0.67 mmol) and solid $Li_2[N_2N_{py}]$ (0.220 g, 0.68 mmol) was added cold (7 °C) benzene (30 mL). The resulting yellow-brown solution was stirred at room temperature for 2 h, becoming dark green during this time. The solution was filtered and the volatiles removed under reduced pressure to leave a green-brown solid. The solid was dissolved in diethyl ether (5 mL) and recrystallized at room temperature over 4 days to provide yellow crystals of **4**. Yield: 0.235 g (45%). Pale yellow crystals of **4** suitable for X-ray diffraction were prepared by recrystallization from a 1:1 hexane/toluene solution at −25 °C over 2 weeks. ^{1}H NMR (CD_2Cl_2, 300.1 MHz, 298 K): 8.84 (2 H, dt, ^3J (*o*-H*m*-H) = 5.0 Hz, ^4J (*o*-H*p*-H) = 1.5 Hz, *o*-NC_5H_5), 8.51 (1 H, d, ^3J (H^6H^5) = 5.7 Hz, H^6), 7.85 (2 × 1 H, 2 × overlapping m, H^4 and *p*-NC_5H_5), 7.58 (1 H, d, ^3J (H^3H^4) = 8.1 Hz, H^3), 7.32 (H, apparent t, apparent J = 5.0 Hz, *m*-NC_5H_5), 7.08 (H, apparent t, apparent J = 6.0 Hz, H^5), 7.06 (2 H, d, ^3J = 7.5 Hz, *m*-$C_6H_3{}^i$Pr$_2$), 6.69 (1 H, t, ^3J = 7.5 Hz, *p*-$C_6H_3{}^i$Pr$_2$), 4.50 (H, broad s, C*H*Me$_2$), 3.84 (2 H, d, ^2J = 12.5 Hz, CH_2), 3.71 (2 H, d, ^2J = 12.5 Hz, CH_2), 1.58 (H, s, Me of N_2N_{py}), 1.28 (12 H, d, ^3J = 6.8 Hz, CH*Me*$_2$), −0.10 (18 H, s, $SiMe_3$). ^{1}H NMR (CD_2Cl_2, 300.1 MHz, 223 K): 8.69 (2 H, broad s, *o*-NC_5H_5), 8.42 (1 H, dd, ^3J (H^6H^5) = 5.7 Hz, ^4J (H^6H^4) = 1.5 Hz, H^6), 7.87 (1 H, overlapping m, H^4), 7.83 (1 H, overlapping t, ^3J = 7.7 Hz, *p*-NC_5H_5), 7.58 (1 H, d, ^3J (H^3H^4) = 8.1 Hz, H^3), 7.31 (2 H, broad s, *m*-NC_5H_5), 7.10 (1 H, apparent t, apparent J = 6.0 Hz, H^5), 7.03 (2 H, d, ^3J = 5.7 Hz, *m*-$C_6H_3{}^i$Pr$_2$), 6.68 (1 H, t, ^3J = 7.7 Hz, *p*-$C_6H_3{}^i$Pr$_2$), 4.96 (1 H, broad septet, ^3J = 6.7 Hz, C*H*Me$_2$), 4.01 (1 H, broad septet, ^3J = 6.6 Hz, C*H*Me$_2$), 3.74 (4 H, 4 x overlapping d, 2 x CH_2), 1.55 (3 H, s, Me of N_2N_{py}), 1.30 (6 H, 2 x broad overlapping d, CH*Me*$_2$), 1.20 (3 H, d, ^3J = 6.6 Hz, CH*Me*$_2$), 1.13 (3 H, d, ^3J = 6.8 Hz, CH*Me*$_2$), −0.12 (9 H, s, Si*Me*$_3$), −0.21 (9 H, s, $SiMe_3$). ^{13}C-{^{1}H} NMR (CD_2Cl_2, 75.5 MHz, 223 K): 164.2 (C^2), 153.6 (*o*-NC_5H_5), 153.0 (*ipso*-2,6-$C_6H_3{}^i$Pr$_2$), 150.0 (C^6), 145.5 (*o*-2,6-$C_6H_3{}^i$Pr$_2$), 142.8 (*o*-2,6-$C_6H_3{}^i$Pr$_2$), 139.3 (C^4), 139.3 (*p*-NC_5H_5), 124.4 (*m*-NC_5H_5), 123.2 (*m*-2,6-$C_6H_3{}^i$Pr$_2$), 122.3 (*m*-2,6-$C_6H_3{}^i$Pr$_2$), 121.6 (C^5), 120.3 (*p*-2,6-$C_6H_3{}^i$Pr$_2$), 119.4 (C^3), 62.4 (*C*H_2-NSiMe$_3$), 61.0 (*C*H_2NSiMe$_3$), 50.7 (*C*(CH_2NSiMe$_3$)$_2$, 27.2 (*C*HMe$_2$), 26.3 (*C*HMe$_2$), 26.3 (CH*Me*$_2$), 26.1 (CH*Me*$_2$), 25.1 (CH*Me*$_2$), 24.0 (Me of N_2N_{py}), 23.7 (CH*Me*$_2$), 0.6 ($SiMe_3$), 0.3 ($SiMe_3$). IR (CsBr plates, Nujol, cm^{-1}): 1615 (m), 1604 (m), 1590 (m), 1574 (w), 1295 (m), 1246 (s), 1156 (w), 1042 (m), 1016 (m), 960 (m), 922 (s), 841 (s), 787 (m), 752 (m), 701 (w), 429 (w), 410 (w) cm^{-1}. Anal. Found (calculated for $C_{32}H_{51}ClN_5Si_2Ta$): C 48.8 (49.4), H 7.0 (6.6), N 8.8 (9.0)%.

[Nb(N^{t}Bu)Cl(N_2N_{py})] (5). [Nb(N^{t}Bu)Cl(N_2N_{py})(py)] (**2**) (0.310 g, 0.53 mmol) was sublimed at 125 °C and 9 × 10^{-6} mbar over 6 h to provide analytically pure [Nb(N^{t}Bu)Cl(N_2N_{py})] (**5**) as a pale yellow solid. Yield: 0.078 g (25%). ^{1}H NMR (C_6D_6, 500.0 MHz, 298 K): 8.92 (1 H, dd, ^3J (H^6H^5) = 5.5 Hz, ^4J (H^6H^4) = 1.0 Hz, H^6), 7.08 (1 H, dd, ^3J (H^4H^5) = 8.0 Hz, ^3J (H^4H^3) = 8.0 Hz, H^4), 6.71 (1 H, d, ^3J (H^3H^4) = 8.0 Hz, H^3), 6.51 (1 H, apparent t, apparent J = 6.7 Hz, H^5), 4.13 (2 H, d, ^2J = 12.5 Hz, CH_2), 3.23 (2 H, d, ^2J = 12.5, CH_2), 1.59 (9 H, s, ^{t}Bu), 0.91 (3 H, s, Me of N_2N_{py}), 0.07 (18 H, s, $SiMe_3$). ^{13}C-{^{1}H} NMR (C_6D_6, 125.7 MHz, 298 K): 159.8 (C^2), 149.1 (C^6), 138.2 (C^4), 121.2 (C^5), 120.7 (C^3), 63.1 (*C*H_2NSiMe$_3$), 46.8 (*C*(CH_2NSiMe$_3$)$_2$), 33.3 (NC*Me*$_3$), 23.8 (Me of N_2N_{py}), 0.5 ($SiMe_3$), not observed: N*C*Me$_3$. IR (NaCl plates, Nujol, cm^{-1}): 1600 (s), 1572 (w), 1358 (s), 1341 (m), 1281 (m), 1245 (s), 1233 (s), 1213 (s), 1157 (w), 1142 (m), 1132 (m), 1116 (m), 1084 (w), 1052 (s), 1048 (s), 1033 (s), 1001 (m), 951 (m), 899 (s), 874 (s), 838 (s), 800 (m), 778 (s), 725 (w), 686 (w), 599 (m), 520 (w), 493 (w), 439 (w) cm^{-1}. Anal. Found (calculated for $C_{19}H_{38}ClN_4NbSi_2$): C 45.0 (45.0), H 7.6 (7.6), N 11.1 (11.1)%.

Crystal structure determination of V(NAr)Cl_2($H_3N'N''N_{py}$)] (1), [Nb(N^{t}Bu)Cl(N_2N_{py})(py)] (2), [Ta(N^{t}Bu)Cl(N_2N_{py})(py)] (3), and [Ta(NAr)Cl(N_2N_{py})(py)] (4). Crystal data collection and processing parameters are given in Table 1. Crystals were mounted in a film of RS3000 perfluoropolyether oil (Hoechst) on a glass fiber and transferred to a Stoë Stadi-4 four-circle diffractometer equipped with an Oxford Cryosystems low-temperature device.[24] Data were collected using $\omega-\theta$ scans with Mo Kα radiation (λ = 0.71073 Å), and absorption and decay corrections were applied to the data as appropriate. Data for **3** were collected on two individual crystals and were scaled and combined. Equivalent reflections were merged, and the structures were solved by direct methods (SIR92[25] or SHELXS-96[26]). Subsequent difference Fourier syntheses revealed the positions of all other non-hydrogen atoms. Structures were refined against F or F^2 using a weighting scheme where appropriate. Corrections for secondary extinction effects were made as necessary.

The crystal of **1** was a very weak diffractor with mean I/σ = 4.79, and hence data were collected only to θ_{max} = 22.5°. The refinement proceeded satisfactorily on 3467 data with (I/σ) > 0 subject to similarity restraints on the C(quaternary)−C(methyl) distances for the ^{t}Bu group

(24) Cosier, J.; Glazer, A. M. *J. Appl. Crystallogr.* **1986**, *19*, 105.
(25) Altomare, A.; Cascarano, G.; Giacovazzo, G.; Guagliardi, A.; Burla, M. C.; Polidori, G.; Camalli, M. *J. Appl. Crystallogr.* **1994**, *27*, 435.
(26) Sheldrick, G. M. *Acta Crystallogr., Sect. A* **1990**, *46*, 467.

Table 1. X-ray Data Collection and Processing Parameters for [V(NAr)Cl_2($H_3N'N''N_{Py}$) (**1**), [Nb(N^tBu)Cl(N_2N_{Py})(py)] (**2**), [Ta(N^tBu)Cl(N_2N_{Py})(py)] (**3**), and [Ta(NAr)Cl(N_2N_{Py})(py)] (**4**)

	1	**2**	**3**	**4**
empirical formula	$C_{27}H_{46}Cl_2N_4SiV$	$C_{24}H_{43}ClN_5NbSi_2$	$C_{24}H_{43}ClN_5Si_2Ta$	$C_{32}H_{51}ClN_5Si_2Ta$
fw	576.63	586.17	674.21	778.37
temp/°C	−123(2)	−123(2)	−123(2)	−123(2)
wavelength/Å	0.71073	0.71073	0.71073	0.71073
space group	*Pbca*	*Pbca*	*Pbca*	$P\bar{1}$
a/Å	14.90(2)	15.586(4)	15.560(5)	10.631(2)
b/Å	16.834(9)	16.593(4)	16.571(4)	10.968(3)
c/Å	24.025(13)	22.303(7)	22.319(6)	16.225(4)
α/deg				94.62(2)
β/deg				96.77(2)
γ/deg				106.06(2)
V/Å^3	6026(1)	5768(2)	5755(3)	1792.6(5)
Z	2	8	8	2
d (calcd)/Mg·m^{-3}	1.27	1.350	1.556	1.44
abs coeff/mm$^-$	0.56	0.61	4.017	3.240
R indices [$I > 2\sigma(I)$][a]	$R_1 = 0.099$, $wR_2 = 0.125$	$R_1 = 0.0605$, $Rw = 0.0654$	$R_1 = 0.0526$, $wR_2 = 0.1215$	$R_1 = 0.0426$, $Rw = 0.0500$
R indices (all data − for refinement on F^2 only)[a]	$R_1 = 0.151$, $wR_2 = 0.161$		$R_1 = 0.0734$, $wR_2 = 0.1446$	

[a] $R_1 = \sum||F_o| - |F_c||/\sum|F_o|$; $wR_2 = \sqrt{\{\sum w (F_o^2 - F_c^2)^2/\sum(w(F_o^2)^2\}}$; $R_w = \sqrt{\{\sum w (|F_o| - |F_c|)^2/\sum(w|F_o|^2\}}$.

C(24)−C(28) and general vibrational restraints on the displacement parameters of the non-H atoms. For all four structures, H atoms bound to carbon were placed in calculated positions and refined in riding models. For **1** the H atoms attached to N(2) and N(4) were located from difference maps and were positionally refined subject to similarity restraints on the N−H distances. The largest peaks and holes in the final Fourier difference syntheses of the tantalum structures **3** and **4** lie less than ca. 1 Å from Ta(1); for **1** the largest peaks were located at 1.54 and 1.40 Å from V(1) and Cl(1), respectively. In all three structures these final peaks and holes are attibuted to residual absorption artifacts.

Crystallographic calculations were performed using SIR92,[25] SHELXS-96,[26] SHELXL-96,[27] or CRYSTALS.[28] A full listing of atomic coordinates, bond lengths and angles, and displacement parameters for **1**−**4** have been deposited at the Cambridge Crystallographic Data Center. See Notice to Authors, Issue No. 1.

Results and Discussion

Initial efforts focused on attempts to prepare vanadium(V) complexes of diamido-pyridine ligands N_2N_{py} or N'_2N_{py} by reaction of the previously described arylimido complex [V(NAr)-Cl_3(THF)][23] with $M_2N_2N_{py}$ or $M_2N'_2N_{py}$ (M = H or Li). Reactions with dilithium derivatives of the diamido-pyridines gave uncharacterized mixtures, and only the reaction of [V(NAr)Cl_3(THF)] with the ligand precursor $H_2N'_2N_{py}$ in cold Et_2O in the presence of Et_3N gave any isolable product at all (eq 1). Under these conditions the vanadium(IV) compound

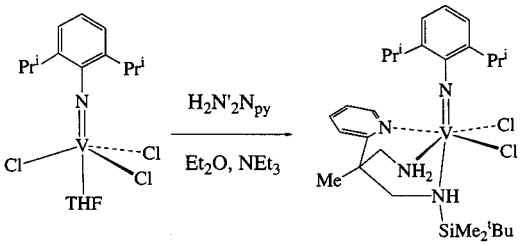

(1)

1

[V(NAr)Cl_2($H_3N'N''N_{py}$)] [**1**, $H_3N'N''N_{py}$ = MeC(2-C_5H_4N)(CH_2-$NHSiMe_2{}^tBu$)(CH_2NH_2)] can be isolated in 12% yield. Attempts to identify any other metal-containing products of this reaction were unsuccessful. Nonetheless, the compound **1** was reproducibly generated, either as red-brown crystals or as a red-brown powder, in similar yields.

The solid-state X-ray structure of [V(NAr)Cl_2($H_3N'N''N_{py}$)] (**1**) is shown in Figures 1a and 1b; selected bond lengths and angles are presented in Table 2. The crystal of **1** was a very weak diffractor but nonethless a full anisotropic refinement of all non-H atoms was possible (subject to vibrational restraints). The H atoms bound the amino nitrogens N(2) and N(4) were located from Fourier difference syntheses and positionally refined.

The X-ray structure of the monomeric unit of **1** (Figure 1a) confirms how the $H_2N'_2N_{py}$ ligand has been substantially altered, with one "arm" still bearing a $SiMe_2{}^tBu$ substituent but with the other having lost this group which has been formally replaced by a hydrogen atom. Together with the presence of a V(IV) center in **1**, this feature is probably indicative of redox reactions taking place during the reaction. The remaining three coordination sites about vanadium are occupied by the arylimido ligand and by a pair of mutually cis disposed chloride ligands. The V=$N_{(imide)}$ distance of 1.685(8) Å is typical for terminal vanadium arylimides (seven examples with V=N distances ranging from 1.615 to 1.730 Å, average 1.693 Å),[29] although it is slightly shorter than the typical range for specifically V(IV)=$N_{(imide)}$ bonds (1.707−1.730 Å for three examples). The V−Cl bond distances are unremarkable.

As mentioned, the hydrogen atoms of the amine donors were located from Fourier difference maps. The V−N(2) bond distance of 2.143(9) Å is typical of V−$N_{(amine)}$ linkages, while the V−N(4) distance of 2.475(9) Å is unusually long, probably due to the strong *trans*-influence of the imido ligand and the large steric bulk of the dimethyl-*tert*-butylsilyl substituent. Interestingly, molecules of **1** form centrosymmetric, hydrogen-bonded dimers in the solid state, in the manner shown in Figure 1b. The hydrogen bonds occur between Cl(2) and H(2A) and between H(2) and Cl(2A). Recent work by Brammer, Orpen, and co-workers has highlighted the widespread occurrence of such M-Cl···H−N bonds in the solid state,[30] and the Cl(2)···

(27) Sheldrick, G. M. *SHELXL-96*; Institut für Anorganische Chemie der Universität Göttingen: Germany, 1996.
(28) Watkin, D. J.; Prout, C. K.; Carruthers, J. R.; Betteridge, P. W. *CRYSTALS*, Issue 10; Chemical Crystallography Laboratory, University of Oxford: Oxford, 1996.
(29) Fletcher, D. A.; McMeeking, R. F.; Parkin, D. "The United Kingdom Chemical Database Service" *J. Chem. Inf. Comput. Sci.* **1996**, *36*, 746. Allen, F. H.; Kennard, O. *Chemical Design Automation News* **1993**, *8*, 1&31.

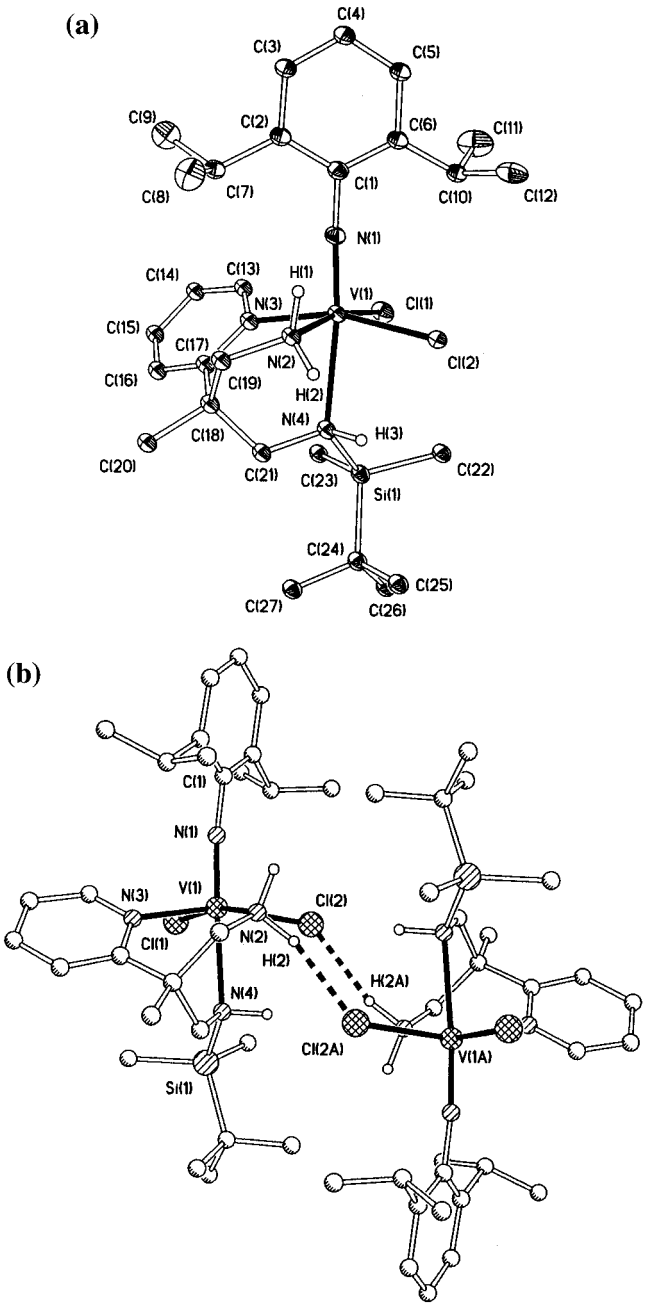

Figure 1. Molecular structure plots of $[V(NAr)Cl_2(H_3N'N''N_{py})]$ (**1**) with carbon-bound H atoms omitted: (a) view of the monomeric unit with displacement ellipsoids drawn at the 40% probability level and N-bound H atoms drawn as spheres of an arbitary radius; (b) ball-and-stick plot of the hydrogen-bonded dimer in which atoms carrying the suffix "A" are related to their counterparts by the symmetry operator $[-x + 1, -y, -z + 2]$.

H(2A) distance of 2.31(3) Å is very close to the median value found for such contacts. It was not possible to establish if molecules of **1** possess a hydrogen-bonded structure in the solution state too since **1** is soluble only in donor solvents such as Et_2O and thf, which would be expected to disrupt any weakly N−H···Cl bonded dimeric structure.

The solid-state structure found by X-ray crystallography is supported by elemental combustion analysis, IR, EPR and NMR spectroscopy, and mass spectromtery. In accordance with the d^1 metal center in **1**, no signals for the complex itself were visible in the ^1H NMR spectrum in the range +30 to −30 ppm. ^1H NMR studies of the reaction mixture nonetheless proved useful, showing signals assigned to $ClSiMe_2{}^tBu$, consistent with the loss of a $SiMe_2{}^tBu$ substituent from $H_2N_2'N_{py}$ and of a chloride ligand from vanadium. The IR spectrum of **1** as a Nujol mull revealed three sharp peaks at 3349, 3236, and 3158 cm^{-1}. Similar absorptions have not been observed in any other metal compound of the N_2N_{py} or N'_2N_{py} ligands. These bands lie in the expected region for N−H stretches and are attributed to the amine hydrogen atoms. The room-temperature EPR spectrum of **1** in thf solution exhibits the expected eight $(2I + 1)$ peaks consistent with a metal-based electron coupling to a quadrupolar vanadium nucleus of nuclear spin $I = {}^7/_2$. With values of $g = 1.982$ and $A = 90.9$ G, the 298 K g-factor and hyperfine coupling parameter are in good agreement with literature values reported for other V(IV) compounds.[31−33]

Table 2. Selected Bond Lengths (Å) and Angles (deg) for $[V(NAr)Cl_2(H_3N'N''N_{Py})]$ (**1**)[a]

distances		angles	
V(1)−N(1)	1.685(8)	V(1)−N(1)−C(1)	173.2(8)
V(1)−N(2)	2.143(9)	N(1)−V(1)−N(2)	93.3(4)
V(1)−N(3)	2.136(9)	N(1)−V(1)−N(3)	96.9(4)
V(1)−N(4)	2.475(9)	N(1)−V(1)−N(4)	168.7(4)
V(1)−Cl(1)	2.374(4)	N(1)−V(1)−Cl(2)	97.9(3)
V(1)−Cl(2)	2.416(4)	N(1)−V(1)−Cl(2)	99.3(3)
N(1)−C(1)	1.38(1)	N(2)−V(1)-N(3)	88.8(4)
Cl(2)···H(2A)	2.31(3)	Cl(1)−V(1)−Cl(2)	93.5(1)
		V(1)−Cl(2) ···H(2A)	132(2)
		N(2)−H(2)···Cl(2A)	169(7)

[a] Atoms carrying the suffix "A" are related to their counterparts by the symmetry operator $[-x + 1, -y, -z + 2]$.

Because of the low yields and ligand degradation associated with the formation of $[V(NAr)Cl_2(H_3N'N''N_{py})]$ (**1**), we turned our attention to the synthesis of N_2N_{py} derivatives of the heavier Group 5 congeners. These metals are typically more resistant to redox processes in their M(V) oxidation states than is vanadium. High-yielding syntheses of Group 4 imido complexes of the N_2N_{py} (**I** and **II**, Chart 1) and N_2N_{am} (**III**, Chart 1) ligands were previously achieved from the reaction of metal imide-containing precursors and the dilithium compounds $Li_2N_2N_{py}$ or $Li_2N_2N_{am}$.[10] Similar routes have been employed in the present work starting from the known[21,22] imido-niobium and -tantalum compounds $[M(NR)Cl_3(py)_2]$ (M = Nb or Ta, R = ^{t}Bu or Ar) and $Li_2N_2N_{py}$ in cold benzene solution. The new compounds $[M(NR)Cl(N_2N_{py})(py)]$ (M = Nb, R = ^{t}Bu **2**; M = Ta, R = N^{t}Bu **3** or Ar **4**) were isolated in fair to good yields, and the reactions are summarized in eq 2.

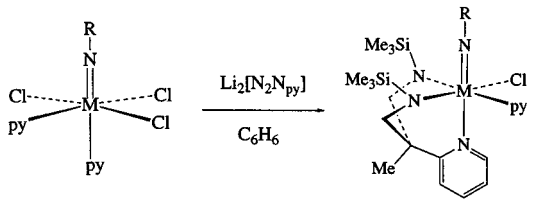

M = Nb, R = ^{t}Bu; M = Ta, R = ^{t}Bu or Ar

M = Nb, R = ^{t}Bu (**2**); M = Ta, R = ^{t}Bu (**3**) or Ar (**4**)

(2)

All three compounds **2**−**4** have been crystallographically characterized. For ease of comparison, views of the three

(30) Aullón, G.; Bellamy, D.; Brammer, L.; Bruton, E. A.; Orpen, A. G. *Chem. Commun.* **1998**, 653.

(31) Dutta, S. K.; Tiekink, E. R. T.; Chaudhury, M. *Polyhedron* **1997**, *16*, 1863.

(32) Wheeler, D. E.; Wu, J.-F.; Maata, E. A. *Polyhedron* **1998**, *17*, 969.

(33) Wen, T.-B.; Shi, J.-C.; Huang, X.; Chen, Z.-N.; Liu, Q.-T.; Kang, B.-S. *Polyhedron* **1998**, *17*, 331.

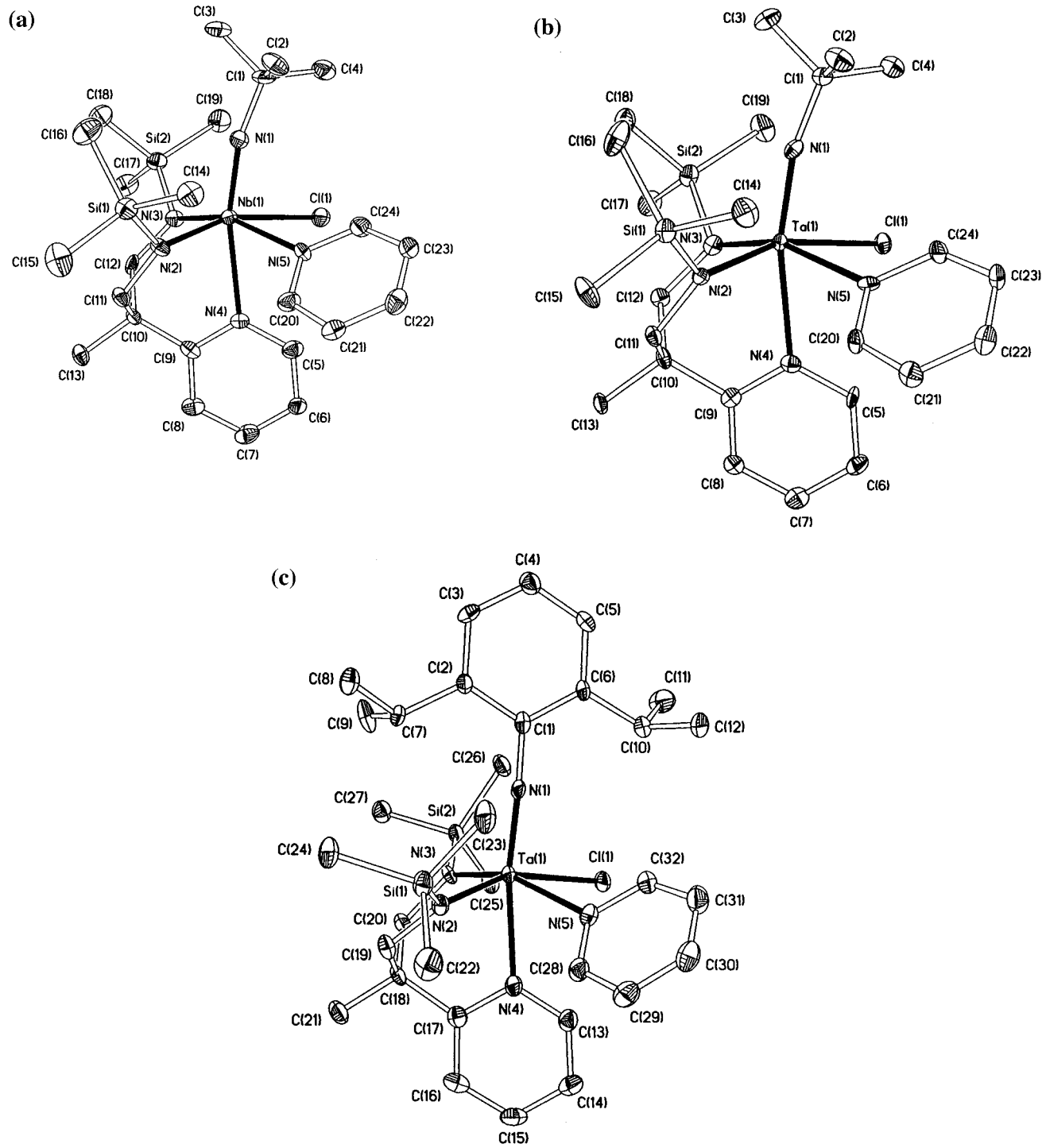

Figure 2. Displacement ellipsoid plots with hydrogen atoms are omitted and ellipsoids drawn at the 45% (**2**, **3**) or 35% (**4**) probability level: (a) [Nb(N^{t}Bu)Cl(N_2N_{py})(py)] (**2**); (b) [Ta(N^{t}Bu)Cl(N_2N_{py})(py)] (**3**); (c) [Ta(NAr)Cl(N_2N_{py})(py)] (**4**).

structures are collected together in Figures 2a−c; selected bond lengths and angles are compiled in Table 3. We shall discussthe three structures together as they form a closely linked series in which the effects of changing the metal from Nb (in **2**) to Ta (in **3**), and then changing the imide N-substituent from ^{t}Bu (in **3**) to Ar (in **4**), can be specifically traced.

The compounds **2**−**4** are the first crystallographically characterized examples of a terminal niobium or tantalum imides supported by a diamide ligand, although monoamide-supported examples such as [Nb(NAr)(NMe_2)$_3$][34] and [Ta(N^{t}Bu)Cl{N($SiMe_3$)$_2$}$_2$][35] are known. They all feature approximately octahedral metal centers with a near-linear organoimido ligand in one of the axial positions. The angles subtended at the imido nitrogen [166.1(5) ≤ C(1)−$N_{(imide)}$−M ≤ 176.6(4)°] show that the imide can in principle act as four-electron donor.[3,36,37] The

(34) Herrmann, W. A.; Baratta, W.; Herdtweck, E. *J. Organomet. Chem.* **1997**, *541*, 445.
(35) Bradley, D. C.; Hursthouse, M. B.; Malik, K. M. A.; Nielson, A. J.; Vuru, G. B. C. *J. Chem. Soc., Dalton Trans.* **1984**, 1069−1072.
(36) Cundari, T. R. *Chem. Rev.* **2000**, *100*, 807.
(37) For leading references on the electron and structural effects of the trans infuence of multiply bonded ligands, and for a theoretical analysis of the bonding in *tert*butyl- and aryl-imido transition metal complexes see: Kaltsoyannis, N.; Mountford, P. *J. Chem. Soc., Dalton Trans.* **1999**, 781.

Table 3. Selected Bond Lengths (Å) and Angles (deg) for [Nb(N^{t}Bu)Cl(N_2N_{Py})(py)] (**2**), [Ta(N^{t}Bu)Cl(N_2N_{Py})(py)] (**3**), and [Ta(NAr)Cl(N_2N_{Py})(py)] (**4**)

parameter	**2** (M = Nb)	**3** (M = Ta)	**4** (M = Ta)
M(1)−N(1)	1.781(6)	1.793(7)	1.822(4)
M(1)−N(2)	2.040(6)	2.043(7)	2.036(4)
M(1)−N(3)	2.044(6)	2.023(8)	2.004(4)
M(1)−N(4)	2.428(5)	2.409(7)	2.397(5)
M(1)−N(5)	2.407(6)	2.370(7)	2.356(4)
M(1)−Cl(1)	2.548(2)	2.518(2)	2.518(1)
N(1)−C(1)	1.464(9)	1.443(11)	1.372(7)
M(1)−N(1)−C(1)	166.1(5)	167.3(6)	176.6(4)
N(1)−M(1)−N(2)	104.2(2)	104.2(3)	103.6(2)
N(1)−M(1)−N(3)	106.8(2)	107.8(3)	104.3(2)
N(1)−M(1)−N(4)	166.4(2)	166.3(3)	171.1(2)
N(1)−M(1)−N(5)	92.3(2)	92.9(3)	96.4(2)
N(1)−M(1)−Cl(1)	91.8(2)	92.1(2)	94.7(1)
N(2)−M(1)−N(3)	92.1(2)	91.9(3)	95.0(2)
N(5)−M(1)−Cl(1)	81.6(1)	82.38(17)	80.7(1)
sum of the angles subtended at N(3)	358(1)	359(1)	360(1)
sum of angles subtended at N(3)	355(1)	354(2)	359(1)

N_2N_{py} ligand adopts a fac-κ^3 coordination mode as found in most of its transition metal imido complexes to date.[8] The pyridyl moiety of N_2N_{py} lies approximately trans to the imido nitrogen, and the Cl and pyridine ligands occupy mutually cis, equatorial positions trans to the amide donors of N_2N_{py}. The angles subtended at the metal between the imido nitrogen N(1) and the donor atoms of the equatorial groups are all in excess of the theoretical 90° expected for a regular octahedral geometry. This is a typical consequence of the trans influence of ligands multiply bonded to transition metals, and the likely electronic and steric driving forces for such features have been dealt with in detail elsewhere.[37]

At 1.781(6) Å, the Nb=$N_{(imide)}$ bond length in **2** is at the long end of the range for alkylimido linkages (range: 1.744(3)−1.789(4) Å for eight *tert*-butylimido complexes).[38−41] The particularly long M=$N_{(imide)}$ bond in **2** (and also in **3** and **4**—see below) is probably a result both of the steric pressure between the imido *tert*-butyl group and the amido trimethylsilyl substituents cis to it and of the presence of strong σ- and π-donor amides in the equatorial positions. The Nb−Cl bond length of 2.548(2) Å is also unusually long, such bonds more commonly lying in the range 2.35−2.45 Å.[29] This presumably reflects a mixture of steric crowding effects and the strong trans influence of the strongly σ- and π-donating N_2N_{py} amide nitrogen donors. Comparison of the Nb−$N_{(pyridine)}$ and Nb−$N_{(pyridyl)}$ bond lengths indicates that the pyridine ligand is marginally more tightly bound to the metal than the N_2N_{py} pyridyl group and, all other factors aside, is consistent with the characteristic trans-bond lengthening effect of imido ligands.[37]

Nearly all of the bond lengths and angles for complex **3** are identical within experimental error to those of **2**, as would be expected from the essentially idential atomic and ionic radii of Nb and Ta.[42] The most notable differences exist in the relative bond lengths of M−$N_{(pyridyl)}$ [2.409(7) Å] and M−$N_{(pyridine)}$ [2.370(7) Å], the pyridine ligand in this compound being noticeably more tightly bound to the metal than the N_2N_{py} pyridyl group. The long M−Cl bond distance of 2.548(2) Å in **2** is shortened to 2.518(2) Å in **3**, although this still remains very long for a terminal Ta−Cl bond, typical values lying nearer to 2.40 Å.[29] The Ta=$N_{(imide)}$ bond distance of 1.793(7) Å is among the longest recorded for a tantalum terminal *tert*-butylimide, previous examples ranging from 1.61(3) Å to 1.78(2) Å.[35,41,43−46]

The same structural motif as in compounds **2** and **3** appears in [Ta(NAr)Cl(N_2N_{py})(py)] (**4**). The Ta=$N_{(imide)}$ bond length of 1.822(4) Å is relatively long compared to those of many other tantalum terminal arylimides, the Ta=N bond lengths of which take values of less than 1.80 Å (1.769(5)-1.799(2) Å for nine examples).[34,38,47−50] As in the tantalum *tert*-butylimido compound **3**, the pyridine ligand is more tightly bound to the metal center than the N_2N_{py} pyridyl group. There is a lengthening of the Ta=NAr bond in **4** compared to Ta=N^{t}Bu in **3**. With the bulky *iso*-propyl ortho-substituents on Ar there is probably a steric origin (at least in part) for this observation. However, a recent comparison of homologous *tert*-butyl and aryl-imido complexes have shown that the M=$N_{(imide)}$ distances in the latter group are, on average, significantly longer and the electronic origins of this have been elucidated.[37,51] There is a general shortening of the other Ta-ligand distances, consistent with the reduced general labilizing effect of arylimides compared to *tert*-butylimides as previously recognized.[37,51]

In the three compounds **2**−**4** the N_2N_{py} amide donor nitrogens N(2) and N(3) are effectively planar [354(2) ≤ {sum of the angles subtended at N(2,3)} ≤ 360(1)°] and so are presumably sp^2 hybridized. Each amide nitrogen can therefore in principle donate 3 electrons to the metal center, depending on the orientation of the amide nitrogen 2p π-donor orbital and the availability of the *n*d (n = 4 or 5) π-acceptor orbitals at metal. For all the compounds the trigonal plane defined by the atoms bonded to each amide nitrogen is twisted by between 46 and 61° out of coplanarity with the best-fit equatorial plane around M as defined by the atoms {N(2), N(3), N(5), Cl(1)}. The effect is to bring the $SiMe_3$ groups out of this equatorial plane and "up" toward the imido ligands. By comparison, the equivalent planes around the amide donors in the five-coordinate Group 4 complexes [M(NR)(N_2N_{py})(py)] (**I**, Chart 1) are much more coplanar.[14] Specifically for M = Zr and R = Ar the least squares planes around the amide nitrogens are angled at only 22.4° and 27.5° from the least-squares equatorial plane around Zr.

There are plausible steric and electronic reasons for the orientation of the amido nitrogen substituents and lone pairs, both operating in the same direction (i.e., that observed in the three crystal structures). On steric grounds one might expect the bulky $SiMe_3$ groups to move out of the equatorial plane to

(38) Williams, D. N.; Mitchell, J. P.; Poole, A. D.; Siemeling, U.; Clegg, W.; Hockless, D. C. R.; O'Neil, P. A.; Gibson, V. C. *J. Chem. Soc., Dalton Trans.* **1992**, 739.
(39) Green, M. L. H.; Michaelidou, D. M.; Mountford, P.; Suárez, A. G.; Wong, L.-L. *J. Chem. Soc., Dalton Trans.* **1993**, 1593.
(40) Stewart, P. J.; Blake, A. J.; Mountford, P. *Inorg. Chem.* **1997**, *36*, 1982.
(41) Bailey, N. J.; Cooper, J. A.; Gailus, H.; Green, M. L. H.; James, J. T.; Leech, M. A. *J. Chem. Soc., Dalton Trans.* **1997**, 3579.
(42) Greenwood, N. N.; Earnshaw, A. *Chemistry of the Elements*; Pergamon Press: Oxford, 1994; p 1141
(43) Nugent, W. A.; Harlow, R. L. *J. Chem. Soc., Chem. Commun.* **1978**, 579.
(44) Jones, T. C.; Nielson, A. J.; Rickard, C. E. F. *J. Chem. Soc., Chem. Commun.* **1984**, 205.
(45) Bates, P. A.; Nielson, A. J.; Waters, J. M. *Polyhedron* **1985**, *4*, 1391.
(46) Chamberlain, L. R.; Steffey, B. D.; Rothwell, I. P.; Huffman, J. C. *Polyhedron* **1989**, *8*, 341.
(47) Chao, Y.-W.; Wexler, P. A.; Wigley, D. E. *Inorg. Chem.* **1989**, *28*, 3860.
(48) Boncella, J. M.; Cajigal, M. L.; Gamble, A. S.; Abboud, K. A. *Polyhedron* **1996**, *15*, 2071.
(49) Cotton, F. A.; Daniels, L. M.; Matonic, J. H.; Wang, X.; Murillo, C. A. *Polyhedron* **1997**, *16*, 1177.
(50) Heinselman, K. S.; Miskowski, V. M.; Geib, S. J.; Wang, L. C.; Hopkins, M. D. *Inorg. Chem.* **1997**, *36*, 5530.
(51) Blake, A. J.; Collier, P. E.; Dunn, S. C.; Li, W.-S.; Mountford, P.; Shishkin., O. V. *J. Chem. Soc., Dalton Trans.* **1997**, 1549.

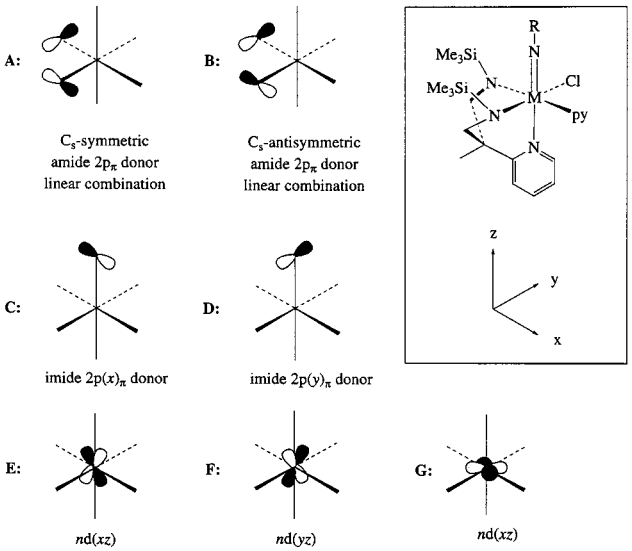

Figure 3. Linear combinations of amide $2p_\pi$-donor orbitals (**A**, **B**), imide $2p_\pi$-donor orbitals (**C**, **D**) and metal based *n*d$_\pi$ ("t_{2g}") orbitals (**E**, **F**, **G**) for [M(NR)Cl(N_2N_{py})(py)] (**2**−**4**) with the orientation of the amide $2p_\pi$ donors idealized to lie in the equatorial plane.

minimize unfavorable interactions with the Cl and pyridine ligands. Presumably there is a limit to how far the $SiMe_3$ groups will be able to rotate before steric interactions with the imido N-substituents inhibit further movemement. Indeed the amido groups in **4** (with the bulkiest imido N-substituent) are rotated by only 46° and 49° out of the equatorial plane around Ta, as might be expected according to steric arguments.

The electronic preferences for rotation of the amide groups can be visualized with reference to Figure 3 which highlights the various metal and nitrogen d$_\pi$ and p$_\pi$ acceptor/donor orbitals. The complexes are taken as being (more or less) oriented with the metal−ligand bonds along Cartesian coordinates and the M═$N_{(imide)}$ vector as being coincident with the *z* axis. In this arrangement there are three σ nonbonding *n*d atomic orbitals at the metal center available for d$_\pi$−p$_\pi$ interactions (Figure 3, **E**, **F**, and **G**). These are the t_{2g} set of orbitals in regular O_h symmetry, namely the *n*d(*xz*), *n*d(*yz*), and *n*d(*xy*) in the C_1 symmetry of **2**−**4**. The metal *n*d(*xz*) and *n*d(*yz*) orbitals will be used for interactions with the 2p(*x*) and 2p(*y*) π-donor orbitals (**C** and **D** in Figure 3) of the imido ligand (the shorter M═$N_{(imide)}$ versus M−$N_{(amide)}$ bond length means that d$_\pi$−p$_\pi$ interactions of the former should take precedent on overlap grounds[52]). Therefore in the molecules **2**−**4** only the metal *n*d(*xy*) is available for $N_{(amide)}$→M π-donation, and for this to occur the appropriate amide p$_\pi$ lone pair donor orbital combination (**A** in Figure 3) clearly should lie in the *x*−*y* (equatorial) plane (note that the anti-symmetric donor orbital linear combination **B** has a node passing through M and so **B** will represent a ligand-based nonbonding orbital). Rotating the amido groups (i.e., the trigonal planes containing the amido nitrogens) out of the equatorial plane will progressively bring the lone pairs into alignment with the remaining *n*d(*xy*) π-acceptor orbital, thus providing an electronic driving force for the features observed in the crystal structures if **2**−**4**. It is clear from this description that the amide nitrogens can act at best as only net 2 electron donors (rather than as 3 electron donors which is in principle possible according to their formal sp^2 hybridization) to the metal center, which in turn possesses a formal valence electron count of 18. A recent computational analysis of the metal−nitrogen bonding in related ene-diamido d^0 metal complexes concurs with the bonding scheme described here for **2**−**4**.[53]

The compounds **2**−**4** have been further characterized by combustion elemental analysis and IR and NMR spectroscopy. The low temperature (218−223 K) NMR spectra are consistent with the solid-state structures shown in Figure 2. In the ^{1}H NMR spectra the $SiMe_3$ groups trans to Cl and pyridine, respectively, appear as two individual singlets, while the CH_2 group protons appear as two pairs of mutually coupled doublets. These features are consistent with the absence of a molecular mirror plane in the ground-state structures. The shifts for the ortho (H^6) protons of the N_2N_{py} pyridyl fragment are consistent with this group being coordinated in solution. All three compounds are fluxional at room temperature in solution. By way of example, the spectra of only [Nb(N^{t}Bu)Cl(N_2N_{py})(py)] (**2**) will be specifically discussed here.

On warming an NMR sample of **2** in CD_2Cl_2 from 218 to 268 K the two $SiMe_3$ group singlets initially broaden and coalesce, and the two pairs of doublets (at 218 K) for the two sets of diasterotopic CH_2 groups of N_2N_{py} broaden and give rise to one pair of mutually coupled doublets (integrating as 2 × 2H). In the fast exchange limit the ^{1}H and ^{13}C NMR spectra of **2** (and also of **3** and **4**) are consistent with the molecule possessing effective C_s symmetry with a mirror plane (on the NMR time scale) passing through the imido, M, and pyridyl groups. A likely mechanism for the exchange process is shown in eq 3. We propose that pyridine dissociates to form C_s-

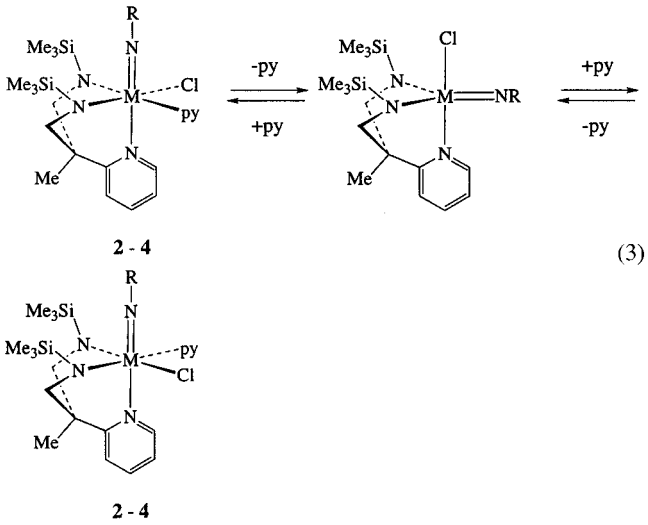

(3)

symmetric [M(NR)Cl(N_2N_{py})] in which the $SiMe_3$ and CH_2 groups can become equivalent; re-coordination of pyridine can occur to give either the initial diasteromer or the mirror image (at right in eq 3), the latter effecting the $SiMe_3$ and CH_2 group exchange implied by the variable temperature NMR spectra. The monomeric, trigonal bipyramidal structures assumed for the intermediates [M(NR)Cl(N_2N_{py})] (with the imido group in the equatorial plane) are based on the known structures of the isoelectronic Group 4 complexes **I** (Chart 1) as well as for the isolated intermediate [Nb(N^{t}Bu)Cl(N_2N_{py})] (**5**—see Equation 4). However, the current results do not conclusively rule out an alternative intermediate with the chloride ligand in the equatorial plane and the imido group trans to pyridyl.

The compound **5** was obtained by careful high-vacuum (10^{-6} mbar) tube sublimation of **2**, and the orientation of the imido group with respect to the other ligands was confirmed by nOe

(52) Zambrano, C. H.; Profilet, R. D.; Hill, J. E.; Fanwick, P. E.; Rothwell, I. P. *Polyhedron* **1993**, *12*, 689.

(53) Galindo, A.; Ienco, A.; Mealli, C. *New J. Chem.* **2000**, *24*, 73.

Table 4. Rate Constants and Activation Parameters for $SiMe_3$ Group Exchange in [M(N^{t}Bu)Cl(N_2N_{Py})(py)] (M = Nb **2** or Ta **3**) (refer to the text for further details)

(a) Results for **3** from ^{1}H NMR line shape analysis:

temperature (K)	avg corrected $\nu_{1/2}$ (Hz)	k_{obs} (s^{-1})	k_{exch} (s^{-1})
262	0.48	1.51	3.02
267	1.00	3.14	6.28
271	2.08	6.54	13.1
275	3.57	11.2	22.4
279	6.30	19.8	39.6
283	10.2	32.0	64.0
287	17.0	53.4	107

$\therefore \Delta H^{\ddagger} = 87.6 \pm 2.3$ kJ mol^{-1}; $\Delta S^{\ddagger} = 99 \pm 10$ J mol^{-1} K^{-1}

(b) Gibbs free energies of activation for **2** and **3** at 268 and 300 K:

For **2**: $\Delta G^{\ddagger}_{(268\ K)} = 53.7 \pm 1.0$ kJ.mol^{-1} (from coalescence measurements)
For **3**: $\Delta G^{\ddagger}_{(268\ K)} = 61.1 \pm 2.5$ kJ mol^{-1} (from Eyring plot $\Delta H^{\ddagger}$ and $\Delta S^{\ddagger}$ values)
$\Delta G^{\ddagger}_{(300\ K)} = 58.0 \pm 2.5$ kJ mol^{-1} (from Eyring plot $\Delta H^{\ddagger}$ and $\Delta S^{\ddagger}$ values)
$\Delta G^{\ddagger}_{(300\ K)} = 61.1 \pm 1.0$ kJ mol^{-1} (from coalescence measurements)

(nuclear Overhauser effect) NMR experiments. Thus irradiation of the *tert*-butyl resonance of **5** gave a strong enhancement of the pyridyl group ortho-H (H^6) resonance. This would only be expected if the N^{t}Bu group were positioned cis to this moiety. The compound **5** is unstable in solution over 24 h, and we were not able to obtain diffraction quality crystals. Addition of pyridine to **5** reforms **2**, consistent with the former being a possible intermediate in the dynamic NMR spectra of **2**. The NMR spectra of **5** are fully consistent with the C_s symmetric, trigonal bipyramidal structure shown in eq 4.

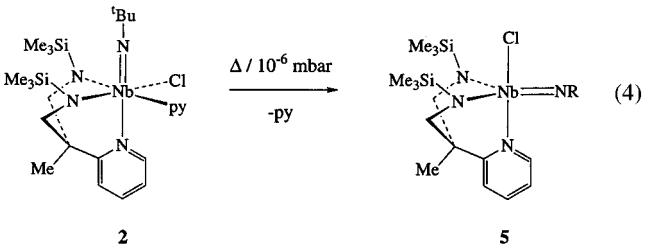

2 **5** (4)

To characterize fully the fluxional processes for [M(N^{t}Bu)-Cl(N_2N_{py})(py)] (M = Nb **2** or Ta **3**) we have determined the associated activation parameters from ^{1}H NMR line shape analyses for **3** (in the slow exchange limit) and coalesence measurements (**2** and **3**) of the inequivalent $SiMe_3$ groups. The closely overlapping nature of the relevant signals for the arylimido analogue **4** prevented us from making a similar study of this system. The results are summarized in Table 4, and Figure 4 shows an Eyring plot for $SiMe_3$ group exchange in **3**.

Activation parameters for $SiMe_3$ group exchange [Ta(N^{t}Bu)-Cl(N_2N_{py})(py)] (**3**) were obtained from ^{1}H NMR spectra of **3** between 262 and 287 K in the slow exchange regime. Curve fitting of the $SiMe_3$ resonances afforded $\nu_{1/2}$ (bandwidth at half-height) values, from which were subtracted the natural line widths as obtained at 218 K to give corrected $\nu_{1/2}$ values. At each temperature, the first-order k_{obs} value was calculated from the average corrected $\nu_{1/2}$ value (Table 4) according to the expression $k_{obs} = \pi \cdot \nu_{1/2}$. Taking chemical *exchange* rate constants (k_{exch}) as $2 \cdot k_{obs}$[54] we obtained the activation parameters listed in Table 4 from the Eyring plot shown in Figure 4. As a check of the reliability of the $\Delta S^{\ddagger}$ and $\Delta H^{\ddagger}$ values obtained from the line shape analysis, we extracted $\Delta G^{\ddagger}_{(300\ K)}$ (Table 4) from ^{1}H coalescence measurements for the $SiMe_3$ resonances (at 300 K)

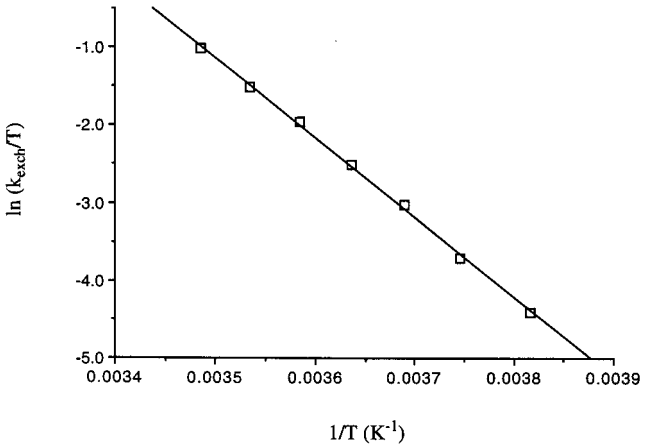

Figure 4. Eyring plot for for $SiMe_3$ group exchange in [Ta(N^{t}Bu)Cl-(N_2N_{py})(py)] (**3**). Refer to the text and Table 4 for further details.

using the standard procedures.[54a] The value of $\Delta G^{\ddagger}_{(300\ K)}$ from coalescence measurements (61.1 ± 1.0 kJ mol^{-1}) compares very well with the value of $\Delta G^{\ddagger}_{(300\ K)}$ (58.0 ± 2.5 kJ.mol^{-1}) calculated from the $\Delta S^{\ddagger}$ and $\Delta H^{\ddagger}$ values from ^{1}H line shape analysis. The sign and magnitude of these parameters are consistent with the exchange mechanism shown in eq 4.[55]

Table 4 also gives the $\Delta G^{\ddagger}_{(268K)}$ values for $SiMe_3$ group exchange for the niobium congener **2**; the corresponding value for **3** was calculated from the $\Delta H^{\ddagger}$ and $\Delta S^{\ddagger}$ data for comparison. The data clearly show that the activation free energy for [M(N^t-Bu)Cl(N_2N_{py})(py)] with M = Ta (**3**, 61.1 ± 2.5 kJ mol^{-1}) is higher than that for Nb (**2**, 53.7 ± 1.0 kJ mol^{-1}). Assuming that the activation entropy $\Delta S^{\ddagger}$ is more or less the same for the exchange processes in **2** and **3**, the differences in $\Delta G^{\ddagger}_{(268K)}$ values reflect differences in enthalpies of activation, $\Delta H^{\ddagger}$. The increase in $\Delta H^{\ddagger}$ from M = Nb to Ta is consistent with the well-known increase in metal−ligand bond strengths down a transition metal triad.[56]

Conclusions

The diamido-pyridine ligands employed in this study provided the key to developing a new class of Group 5 imido complexes. While the synthesis of vanadium complexes was hampered by ligand degradation and redox side-reactions, a series of niobium

(54) (a) Sandström, J. *Dynamic NMR Spectroscopy*; Academic Press: London, 1992. (b) Green, M. L. H.; Wong, L.-L.; Sella, A. *Organometallics* **1992**, *11*, 2660.

(55) Wilkins, R. G. *Kinetics and Mechanism of Reactions of Transition Metal Complexes*; VCH: Weinheim, 1991.

(56) Mingos, D. M. P. *Essential Trends in Inorganic Chemistry*; Oxford University Press: Oxford, 1998.

and tantalum imido complexes was prepared and structurally characterized; the solution dynamics of the new complexes were fully analyzed, and one potential intermediate in these processes was isolated. Future studies on these systems will concentrate on the reaction chemistry supported by the new diamido-pyridine-imide ligand sets.

Acknowledgment. We thank Dr. P. A. Cooke for help with the X-ray data collection. We also thank the Deutsche Forschungsgemeinschaft, the Engineering and Physical Sciences Research Council, the Leverhulme Trust, the Fonds der Chemischen Industrie, the Royal Society, the DAAD, and the British Council for financial support.

Supporting Information Available: X-ray crystallographic files in CIF format for the structure determinations of **1**, **2**, **3**, and **4**. This material is available free of charge via the Internet at http://pubs.acs.org.

IC0102541